Collective oscillations of the superconducting gap of multilayered Josephson junctions

S. E. Shafranjuk* and J. B. Ketterson
Department of Physics and Astronomy, Northwestern University, Evanston, Illinois 60208, USA
(Received 19 September 2005; revised manuscript received 21 October 2005; published 13 December 2005)

Collective modes involving the gap amplitude Δ and phase Φ in a multilayered superconducting junction are considered. The junction is formed by a sequence of "clean" superconducting layers *S* separated by insulating barriers *I*. Using the quasiclassical Green function method, we derive the self-consistent linear equations describing the collective amplitude δ and phase φ oscillations. We find that the δ and φ modes in "clean" multilayered Josephson junctions may be long lived for a range of magnitudes of the barrier transparency and Cooper coupling strength. We find that the frequency of the resonances in a multilayered junction can be tuned by applying a bias supercurrent across the adjacent subjunction.

DOI: 10.1103/PhysRevB.72.212506 PACS number(s): 74.81.Fa, 74.50.+r, 74.78.Fk

The collective modes (CM) of multilayered superconductors are of a fundamental interest. In a bulk BCS superconductor, with a complex energy gap given by $\Delta=|\Delta|e^{i\Phi}$, two modes have been discussed, one involving a small oscillation $\varphi(t)$ of the phase, $\Phi(t)=\Phi_0+\varphi(t)$, and the other an oscillation $\delta(t)$ of the gap amplitude, $|\Delta(t)|=\Delta_0+\delta(t)$ near their steady state values Φ_0 and Δ_0, where t is the time variable. The first of these, which is referred to as the Anderson-Bogoliubov (AB) mode,[1,2] would occur at the electron plasma frequency ω_p (typically in metal superconductors $\omega_p/\varepsilon_F\approx 10$, $\Delta/\varepsilon_F\approx 10^{-3}-10^{-4}$, and the Fermi energy $\varepsilon_F\approx 1$ eV): an oscillating phase necessarily produces an oscillating current which in turn creates an oscillating charge density.[3] The second mode, which was examined by Littlewood and Varma[4] (LV), is found to lie at or above the absorption threshold 2Δ, and hence is strongly damped.[5]

In the SIS Josephson junction sketched in Fig. 1 (where *S* and *I* denote superconductors and an insulator, respectively) one expects symmetric (+) and antisymmetric (−) AB and LV modes $\omega_{AB}^{\pm}$ and $\omega_{LV}^{\pm}$. The branches ω_{AB}^{+} and $\omega_{LV}^{\pm}$ lie near ω_p and 2Δ, respectively. In low transparent junctions $\omega_{LV}^{\pm}$ strongly decay,[7] while the ω_{AB}^{-} mode is typically stable (since $\omega_{AB}^{-}<2\Delta$) and actually coincides with the Josephson plasma mode, i.e., $\omega_{AB}^{-}=\omega_{JP}=\sqrt{2eI_c/\hbar C}$, where I_c and C are the junction critical current and capacitance, respectively. The ω_{JP} mode arises due to ac Josephson supercurrent oscillations, which are out of phase with the ac charge on the junction's electrodes. However, if the junction transparency D is not low ($D\leqslant 1$), the situation may be dramatically different. The modes $\omega_{LV}^{\pm}$ can then be pushed down by a stronger tunneling interaction and may become stable. All the relevant modes (i.e., $\omega_{LV}^{\pm}$ and ω_{AB}^{-}) then interact with each other, which means that the Josephson supercurrent oscillations are hybridized with oscillations involving elementary Cooper pairing processes.

The Josephson supercurrent across a "clean" SIS junction is transferred as follows (see Fig. 1). A Cooper pair in the left *S* layer can dissociate into a lone electron in *S* and an electron which enters the right S electrode. This electron then joins the superfluid condensate, but to conserve charge, a hole *h* is simultaneously created; momentum conservation requires that this hole moves opposite to the incident electron *e*. The hole (which has a negative energy $-\Delta$) is reflected back to the left *S* electrode, and, on entering the left electrode, annihilates with the remaining electron of the original Cooper pair, as shown in Fig. 1. The duration of the whole process is $\leqslant\min\{\hbar/\omega_{JP},\hbar/\Delta\}$, which ensures that a Cooper pair is coherently transferred across the junction.

In a multijunction structure[6–8] one expects additional modes. Of particular interest may be a symmetric SISIS structure, where, for example, we expect two Josephson plasma modes $\omega_{JP}^{\pm}$ which are symmetric (+) and antisymmetric (−) with respect to the central superconducting layer.

Many methodologies to calculate collective mode frequencies are available. For a clean superconductor one can use the time-dependent Bogoliubov equations,[9] from which a Green function of the system is computed. One assumes an oscillating order parameter and perturbatively calculates the change of the Bogoliubov wave function $\hat{\Psi}=\hat{\Psi}_0+\hat{\Psi}_1$. $\hat{\Psi}_0$ and $\hat{\Psi}_1$ are then used to calculate the change in the gap function via a self-consistency condition.[10]

In this paper collective oscillations and a relationship between them in highly transparent SIS and SISIS superconducting junctions are considered. We analyze two kinds of processes: (i) those involving creation and recombination of Cooper pairs, which depend on the coupling constant λ, and

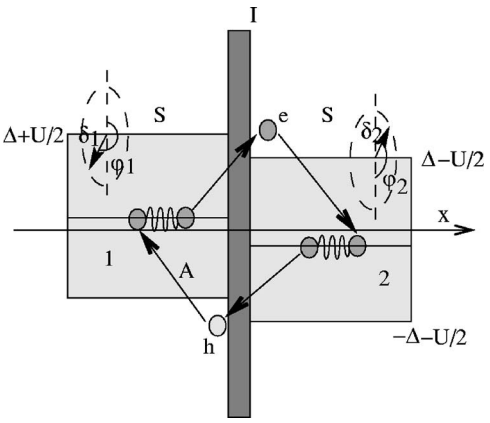

FIG. 1. A Cooper pair transfer across an SIS junction. $U=(\hbar/2e)\dot{\varphi}_a$ is a small ac bias voltage due to the JP oscillations.

(ii) those involving the junction capacitance C and ac supercurrents. The paper is organized as follows. First we determine the equilibrium Bogoliubov state $\hat{\Psi}$ of the system. For the case of the SIS junction we then assume that the system is disturbed by small nonstationary deviations $\varphi^{(1,2)}(t)$ and $\delta^{(1,2)}(t)$ where the upper subscripts denote the two adjacent electrodes. The steady state $\hat{\Psi}_0$ and a nonstationary perturbation $\hat{\Psi}_1(t)$ are then used to compute the quasiclassical retarded one-point Green function $\hat{g}$ of the junction.

The Bogoliubov state $\hat{\Psi}$ of the system (which is a spinor with two components u and v) is found using the quasiclassical approach[11–13] for envelope wave functions $\hat{\psi}$. A small nonstationary deviation of the envelope wave function $\hat{\psi}_1=\hat{\psi}-\hat{\psi}_0$ is then described by the linearized matrix Andreev equation,

$$i\frac{\partial}{\partial t}\hat{\psi}_1=\mathcal{H}_0\hat{\psi}_1+\mathcal{H}_1\hat{\psi}_0, \tag{1}$$

where we write $\hat{\psi}_1$ and $\hat{\psi}_0$ in spinor form as

$$\hat{\psi}_0=\begin{pmatrix}u_0\\ v_0\end{pmatrix},\quad \hat{\psi}_1=\begin{pmatrix}u_1\\ v_1\end{pmatrix}. \tag{2}$$

Here $\mathcal{H}_0$ is the unperturbed Hamiltonian,

$$\mathcal{H}_0=\begin{pmatrix}-\varepsilon+\kappa v_F q & -i\Delta_0\\ i\Delta_0 & -\varepsilon-\kappa v_F q\end{pmatrix}, \tag{3}$$

where $\kappa=v_x/v_F$, v_F is the Fermi velocity, v_x is the x component of the velocity, $q=\xi_\varepsilon/v_F$ is the envelope wave vector, $\xi_\varepsilon=(\sqrt{\varepsilon^2-\Delta_0^2}\,\mathrm{sign}\,\varepsilon+i\delta)\theta(\varepsilon^2-\Delta_0^2)+i\sqrt{\Delta_0^2-\varepsilon^2}\theta(\Delta_0^2-\varepsilon^2)$, $\theta(x)$ is the Heaviside step function; $\mathcal{H}_1$ is a small time-dependent perturbation induced by the CM's

$$\mathcal{H}_1=\begin{pmatrix}eU & -i(\delta-i\varphi\Delta_0)\\ i(\delta+i\varphi\Delta_0) & -eU\end{pmatrix}. \tag{4}$$

The coupling between the two junction electrodes in Eqs. (1), (3), and (4) is taken into account in two ways: (i) via "special" boundary conditions[12,13] for the envelope wave function $\hat{\psi}$ and (ii) via the Josephson relationship[14] $\dot{\varphi}^{(1)}-\dot{\varphi}^{(2)}=(2e/\hbar)U$, where U is a small oscillatory bias voltage induced by the CM. All the functions in (1), (3), and (4) depend on the coordinate along the quasiclassical trajectory x. The functions u_1, v_1, δ, and φ are also time dependent. Equation (1) is valid under the assumption $\hbar v_F q \ll E_F$ (which actually defines quasiclassical motion[11–13]); here q is the *envelope* wave vector characterizing "slow" variations of the physical quantities along the quasiclassical trajectory (typically $q\sim\pi/\xi_S$, where ξ_S is the BCS coherence length in S), and E_F is the Fermi energy. Equation (1) is completed by the linearized equations for δ and φ, which follow from the self-consistency condition for the energy gap and the continuity condition for the electric current and at zero temperature take the form,

$$\delta_{s(a)}=\lambda\langle \mathrm{Re}\, f_1^{s(a)}\rangle_{\varepsilon,n} \tag{5}$$

$$\Delta_0\ddot{\varphi}_{s(a)}=\lambda\langle \mathrm{Im}\,\ddot{f}_1^{s(a)}\rangle_{\varepsilon,n}+\omega_{J0}^2\langle\kappa g_1^{s(a)}\rangle_{\varepsilon,n}, \tag{6}$$

where λ is the Cooper coupling constant, $\langle\ldots\rangle_{\varepsilon,n}=\int d\Omega_n\int d\varepsilon(\cdots)/(4\pi)$ (with $\mathbf{n}=\mathbf{p}/p_F$, where $\mathbf{p}$ is the electron momentum), $\omega_{J0}^2=\pi\Delta_0/(R_N C)$, $R_N=1/(e^2 v_F \nu_0 D)$ (the normal state junction resistance), ν_0 is the electron density of states at the Fermi level, $f_1=\mathrm{Tr}\{\hat{P}_n\hat{g}_1\}$, and $g_1=\mathrm{Tr}\{\hat{P}_d\hat{g}_1\}$; $\hat{P}_n$ and $\hat{P}_d$ are projection operators defined by $\hat{P}_n=(\hat{\tau}_1+i\hat{\tau}_2)/2$ and $\hat{P}_d=(\hat{1}+\hat{\tau}_3)/2$, where the Pauli matrices are $\hat{\tau}_i$; $i=1\cdots3$ and g_1 and f_1 are discussed below. The indices $s(a)$ in Eqs. (5) and (6) denote symmetric (s) and antisymmetric (a) combinations of the form $\delta_{s(a)}=(\delta^{(1)}\pm\delta^{(2)})/\sqrt{2}$, etc. in the two adjacent electrodes one and two. The two terms on the right-hand-side of Eq. (6) have different physical origins. The first term follows from the self-consistency condition for $\Delta(t)$ and the second term is related to the Josephson plasma oscillations described by the continuity condition for the CM-induced ac electric current. The functions g_1 and f_1 entering Eqs. (5) and (6) are small corrections to the quasiclassical Green function matrix, and are computed using the solutions for u_1 and v_1 obtained from Eq. (1) which satisfy the boundary conditions for a junction of a particular geometry. Following Refs. 11–13 we write

$$\hat{g}_1=(\bar{\psi}_0^-\psi_0^+)^{-1}(\psi_0^+\bar{\psi}_1^-+\psi_0^-\bar{\psi}_1^++\psi_1^+\bar{\psi}_0^-+\psi_1^-\bar{\psi}_+^0), \tag{7}$$

where $\bar{\psi}=-i\psi^T(\hat{\tau}_2)$ and the superscript "T" means transpose. The envelope spinor wave functions $\psi_1^\pm(x)$ [as well as $\psi_0^\pm(x)$], which are solutions of Eq. (1), satisfy the boundary conditions $\psi_1^+(x)\to0$ at $x\to+\infty$ and $\psi_1^-(x)\to0$ at $x\to-\infty$. From Eqs. (1), (3), and (4) one finds

$$\hat{\psi}_1^{(1,2)}(x,\kappa)=\hat{Y}^{(1,2)}(\kappa)\hat{\psi}_0^{(1,2)}(x,\kappa), \tag{8}$$

where the upper indices 1 and 2 indicate, the left and right electrodes, and

$$\hat{Y}^{(1,2)}=\delta^{(1,2)}\hat{G}^{(1,2)}+\varphi^{(1,2)}\hat{H}^{(1,2)}+\varphi^{(2,1)}\hat{K}^{(1,2)}. \tag{9}$$

The intraelectrode dynamics arise from the auxiliary functions $\hat{G}^{(2)}=2(-i\hat{\tau}_1(\varepsilon-\omega)+\kappa\xi_\varepsilon\hat{\tau}_2+\Delta_0\hat{\tau}_3)/D_0$, $\hat{G}^{(1)}=-\hat{\tau}_3\hat{G}^{(2)}$, $\hat{H}^{(2)}=[i(\omega(\varepsilon-\omega)+2\Delta_0^2)\hat{1}+i\omega\kappa\xi_\varepsilon\hat{\tau}_3-2\Delta_0\kappa\xi_\varepsilon\hat{\tau}_1+\Delta_0(\omega-2\varepsilon)(i\hat{\tau}_2)]/D_0$, and $\hat{H}^{(1)}=-\hat{\tau}_3\hat{H}^{(2)}$, while the interelectrode coupling is due to the terms $\hat{K}^{(2)}=\omega(i(\omega-\varepsilon)\hat{1}-i\kappa\xi_\varepsilon\hat{\tau}_3+\Delta_0(i\hat{\tau}_2))/D_0$ and $\hat{K}^{(1)}=-\hat{\tau}_3\hat{K}^{(2)}$; here $D_0=2\omega(2\varepsilon-\omega)$ and ω is the frequency variable; the expressions for these functions are rather cumbersome and were obtained using computer algebra.

As noted above, the envelope wave function is obtained by applying special boundary conditions at the interface barrier matching $\psi_\pm^{(1,2)}(x_B)$ (where x_B is the coordinate of the interface barrier) in adjacent electrodes. Using $\psi_\pm^{(1,2)}(x)$, one computes the steady-state retarded Green function $\hat{g}_0(\varepsilon,x)$, which determines the static properties of the junction.

Using Eqs. (7), (8), and (9), we can reduce Eqs. (5) and (6) to a linear matrix equation,

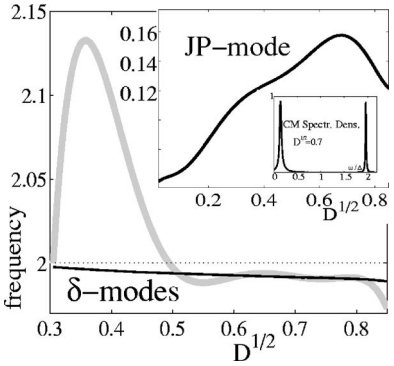

FIG. 2. Josephson plasma oscillation (JP) and δ-mode branches in an SIS junction. The solid lines show stable branches while a gray thick line corresponds to an unstable branch. The inset shows a detailed view of the JP branch.

$$[\hat{\Upsilon}(\omega) - \hat{1}]\hat{\beta} = 0; \tag{10}$$

here $\hat{\beta}$ is a $4\times n$-component vector (n being the number of interfaces) and $\hat{\beta}^T = (\delta_a, \varphi_a, \delta_s, \varphi_s)$. The condition $\det\|\hat{\Upsilon}(\omega, D) - \hat{1}\| = 0$ yields the characteristic equation for the CM frequencies ω_{AB}^- and $\omega_{LV}^{\pm}$.

The coupling between different ω_{AB}^- and $\omega_{LV}^{\pm}$ modes is proportional to λ and ω_{J0}^2. As follows from Eqs. (5) and (6), a strong renormalization of the Josephson plasma frequency by the superconducting order parameter oscillations occurs if the symmetric ω_{LV}^+ mode decays and $(\lambda/\Delta_0)\Xi_a \simeq 1$ [where $\Xi_a = \partial(\mathrm{Im}\langle f_1^a\rangle_{\varepsilon,n})/\partial\varphi_a$, and $f_1^a = f_1^{(1)} - f_1^{(2)}$]. The decay of the ω_{AB}^- and $\omega_{LV}^{\pm}$ modes is determined by a balance between the ac quasiparticle tunneling current and the cos φ component of the ac supercurrent.

The modes ω_{AB}^- and $\omega_{LV}^{\pm}$ are obtained as numerical solutions of Eq. (10) and are calculated versus the barrier transmission coefficient $t = \sqrt{D}$, Cooper coupling constant λ, and ω_{J0} (this latter quantity coincides with the usual Josephson plasma frequency ω_{JP} of a low-transparency SIS junction at zero temperature). In Fig. 2 we plot the results calculated for the SIS junction for $\lambda = 0.3$ and $\omega_{J0} = 0.5$ versus the barrier transmission coefficient $t = \sqrt{D}$. The stable branches are shown as solid lines (along which the dissipation vanishes) while a strongly decaying mode is indicated by a thick gray line. The main part of Fig. 2 shows the $\omega_{LV}^{\pm}$ modes. A stable branch ω_{LV}^- exists for $t \geqslant 0.3$ and is located slightly below 2Δ. The ω_{LV}^- width is $\gamma_{LV}^- = 0.003\Delta$. Another branch ω_{LV}^+, with the width $\gamma_{LV}^+ = 0.015$, is less stable and is strongly frequency dependent. The Josephson plasma (JP) mode originating from the ac Cooper pair transfer across the junction[15] is shown schematically in inset to Fig. 2. The corresponding CM spectral density computed for $t = 0.4$ (see the other inset to Fig. 2) shows two sharp peaks at $\omega = 0.12$ and $\omega = 1.98$ in units of Δ.

The ω_{AB}^- and $\omega_{LV}^{\pm}$ modes have a more complicated structure in multilayered junctions consisting of several barriers. In Fig. 3 we show a double barrier SISIS junction, where we assume that the bias across each SIS subjunction may be applied *independently*.[16,17] Since the middle S electrode in the SISIS junction is common to both SIS subjunctions, the two junctions couple to each other. A particular effect of such a coupling is manifested as the *splitting* of the φ and δ modes belonging to each subjunction. In Fig. 4 we show the calculated results for the eigenfrequencies ω_{AB}^- and $\omega_{LV}^{\pm}$ versus the middle-layer thickness d (in units of the BCS coherence length ξ). One can see six branches. For the case $t = 0.8$, $\lambda = 0.3$, all the branches (indicated by solid lines) are stable with width $\gamma = 0.005$. The eigenfrequencies ω_{AB}^- and $\omega_{LV}^{\pm}$ of the mode localized near the left barrier depend on the steady state phase difference Φ_0^R applied across the right barrier as shown in inset to Fig. 3. One can see that the position of CM branches versus Φ_0^R *can be shifted by* $\sim 30\%$. If the transparency of interface barriers I_1 and I_2 in an SI_1SI_2S junction is different, the junction asymmetry results in additional splitting which remains finite, though the middle S layer is very thick (see dotted lines in Fig. 4 plotted for $t_1 = 0.75$ and $t_2 = 0.85$).

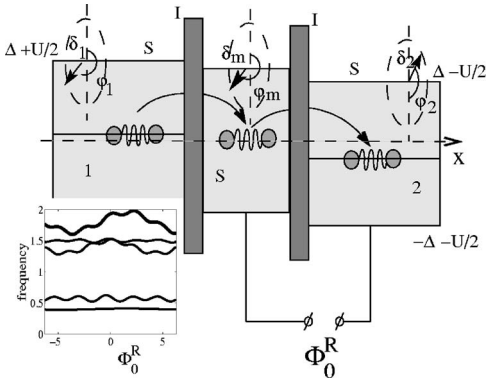

FIG. 3. The Cooper pair transfer across the SISIS junction. Φ_0^R is the steady state phase difference across the right SIS subjunction. The inset shows the CM branches versus Φ_0^R.

The CM discussed in this paper may be observed experimentally in highly transparent SIS and SISIS tunneling junctions as resonances in the real and imaginary parts of the complex ac impedance $Y_{ac}(\omega)$ versus frequency ω. The func-

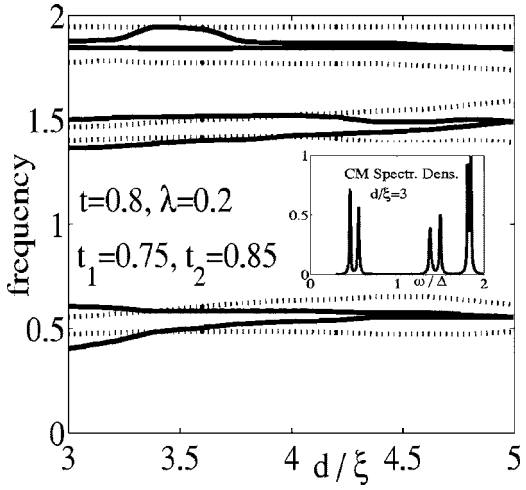

FIG. 4. The CM branches in the SISIS junction (solid lines). Dotted lines show the CM branches in an asymmetric SI_1SI_2S junction.

tions $\mathrm{Re}\{Y_{\mathrm{ac}}(\omega)\}$ and $\mathrm{Im}\{Y_{\mathrm{ac}}(\omega)\}$ are out of phase with each other and are determined by the ac Josephson and quasiparticle currents. The δ and φ modes can be distinguished further by applying a dc magnetic field in parallel to the junction. We conclude that the collective oscillations of the superconducting gap amplitude and phase in "clean" multilayered Josephson junctions may be long lived for appropriate magnitudes of the barrier transparency D and Cooper coupling constant λ. The frequencies of these sharp resonances in a multilayered junction may be tuned by applying a bias supercurrent across the adjacent subjunction.

This work was supported by the National Science Foundation under Grant No. EIA-0218652.

*URL: http://pubweb.northwestern.edu/~ssh192

[1] P. W. Anderson, Phys. Rev. **112**, 1900 (1958).

[2] N. N. Bogoliubov, V. V. Tolmachev, and D. V. Shirkov, *A New Method in the Theory of Superconductivity* (Consultants Bureau, Inc., New York, 1959).

[3] A. Bardasis and J. R. Schrieffer, Phys. Rev. **121**, 1050 (1961).

[4] P. B. Littlewood and C. M. Varma, Phys. Rev. B **26**, 4883 (1982).

[5] A. J. Leggett, Prog. Theor. Phys. **36**, 161 (1966).

[6] L. N. Bulaevskii, Sov. Phys. JETP **37**, 1133 (1973); L. N. Bulaevskii, M. P. Maley, and M. Tachiki, Phys. Rev. Lett. **74**, 801 (1995); L. N. Bulaevskii, V. L. Pokrovsky, and M. P. Maley, *ibid.* **76**, 1719 (1996).

[7] W. C. Wu and A. Griffin, Phys. Rev. Lett. **74**, 158 (1995); W. C. Wu and A. Griffin, Phys. Rev. B **51**, 15317 (1995); W. C. Wu and A. Griffin, Phys. Rev. B **52**, 7742 (1995).

[8] S. E. Shafranjuk, M. Tachiki, and T. Yamashita, Phys. Rev. B **53**, 15136 (1996); S. E. Shafranjuk, M. Tachiki, and T. Yamashita, Phys. Rev. B **55**, 8425 (1997); S. E. Shafranjuk, M. Tachiki, and T. Yamashita, Phys. Rev. B **57**, 582 (1998).

[9] J. B. Ketterson and S. N. Song, *Superconductivity* (Cambridge University Press, Cambridge, 1998).

[10] I. P. Nevirkovets and S. E. Shafranjuk, Phys. Rev. B **59**, 1311 (1999).

[11] A. V. Svidzinsky, *Space-inhomogeneous Issues of the Superconducting Theory* (Science, Moscow, 1982, in Russian).

[12] A. Shelankov and M. Ozana, Phys. Rev. B **61**, 7077 (2000).

[13] A. V. Zaitsev, Zh. Eksp. Teor. Fiz. **86**, 1742 (1984); A. V. Zaitsev, Sov. Phys. JETP **59**, 1015 (1984).

[14] K. K. Likharev, *Dynamics of Josephson Junctions and Circuits* (Gordon and Breach, New York, 1986).

[15] A. Furusaki and M. Tsukada, Phys. Rev. B **43**, 10164 (1991); C. W. J. Beenakker and H. van Houten, Phys. Rev. Lett. **66**, 3056 (1991).

[16] I. P. Nevirkovets, O. Chernyashevskyy, and J. B. Ketterson, IEEE Trans. Appl. Supercond. **15**, 129 (2005); I. P. Nevirkovets, O. Chernyashevskyy, and J. B. Ketterson, J. Appl. Phys. **97**, 123903 (2005).

[17] S. Russo, M. Kroug, T. M. Klapwijk, and A. F. Morpurgo, Phys. Rev. Lett. **95**, 027002 (2005).